# Stimulated Compton Scattering in Two-Color Ionization of Hydrogen with keV Electromagnetic Fields

H. Bachau
*Centre des Lasers Intenses et Applications CNRS-CEA-Université de Bordeaux, 351 Cours de la Libération, Talence F-33405, France*

M. Dondera, and V. Florescu
*Faculty of Physics and Centre for Advanced Quantum Physics, University of Bucharest, RO-077125 Bucharest-Măgurele, Romania*

(Received 28 August 2013; published 19 February 2014)

We present a theoretical study of two-color ionization of hydrogen with keV photons at intensities ranging from $10^{16}$ to $10^{18}$ W/cm$^2$. We consider the atom in interaction with a superposition of two electromagnetic pulses centered around two frequencies that differ by a few atomic units and we present in detail the case of the frequencies 55 and 50 a.u. We present the electron energy spectra, angular distributions, and ionization rates based on nonperturbative and perturbative calculations. Although the ejected electron energy distribution is dominated by one-photon ionization from each pulse, we are able to identify the contribution of stimulated Compton scattering, a process in which one photon is absorbed while the other is emitted, the photon energy difference being transferred to the electron. This leads to low-energy electrons, and we show in particular that it is of crucial importance to consider the retardation effects on the ionization rates and the electron angular distributions. The relative propagation direction of the two fields also plays an important role; in the case of counterpropagating fields, the ionization by stimulated Compton scattering is dominated by $\mathbf{A}^2$ and competes with one-photon ionization at high intensities.

DOI: 10.1103/PhysRevLett.112.073001 PACS numbers: 32.80.Rm, 32.30.Rj, 32.80.Fb

The rapid development of free-electron lasers (XFELs) delivering x rays of high intensity and femtosecond (fs) pulse duration [1–4] opens the pathway to study quantum effects in the x-ray regime. The XFELs are expected to provide intensities of about $10^{17}$-$10^{19}$ W/cm$^2$, where the observation of nonlinear processes with keV photons becomes feasible. For example, the nonlinear atomic response to intense x rays has been identified in neon [5], at a photon energy of 1 keV and an intensity of the order of $10^{17}$ W/cm$^2$. More recently, deep inner shell multiphoton ionization of xenon, at a photon energy of 5.5 keV, has been observed at the SACLA facility in Japan [6]. A major advance in this domain is the extension of optical wave-mixing techniques to the x-ray domain. Controlled delay two-color x-ray fs pulses with a relative delay ranging from 0 to 40 fs and photon energies close to 1.5 keV have been produced [7], with a color separation of the order of 30 eV.

In addition to the fundamental applications of two-color pulses in time-domain spectroscopy, their use yields information on less-studied two-photon processes. We show in the following that the electron energy distributions in the ionization of a ground state hydrogen atom, due to the interaction with the superposition of two pulses of electromagnetic radiation, reveal a peak corresponding to an ionization process where the bound electron absorbs the photon energy difference. This process is energetically allowed provided that the atomic ionization potential is smaller than the color separation, We identify this contribution as due to stimulated Compton scattering (SCS). Compton scattering is one of the ionization mechanisms of atoms, explained by the simultaneous absorption of one photon and the spontaneous emission of a lower-energy photon. In our case, the presence of photons with a frequency lower than the absorbed one stimulates the emission at this particular frequency. It is worthwhile to note that our context differs from that first proposed by Schrödinger [8], Kapitza and Dirac [9], also referred to as SCS, which addresses the particular case of electron beams in interaction with standing light waves. Here, we describe the scattering of a two-color pulse of electromagnetic radiation by a bound electron.

The numerical results presented in this Letter for the electron energy and angular distributions in two-color ionization of hydrogen correspond to photon energies close to 1.5 keV and intensities of the order of $10^{16}$-$10^{18}$ W/cm$^2$. Our results are obtained by resolving the time-dependent Schrödinger equation (TDSE) [10]. It is worth noting that, at the photon energies $\omega$ and the intensities considered here, the ratio of the ponderomotive energy (the quiver energy of the electron in the electromagnetic field, $U_p = I/4\omega^2$) and the photon energy is much less than 1. At the same time, the value of the Keldysh parameter [11], given by $\sqrt{I_p/2U_p}$ (where $I_p$ is the atomic ionization potential), is much greater than 1, unfavorable for tunnel ionization. Given the values of these two parameters, it makes sense to compare our results with lowest order perturbation theory (LOPT) calculations.

 

At first sight, retardation effects are not expected to play an important role for a few keV photons. Nevertheless, theory and experiment reveal a different situation in the photoionization of atoms and more complex systems [12,13]. In our recent theoretical studies devoted to retardation effects in the one- and two-photon ionization of hydrogen [10,14,15] in the context of a one-color pulse, we have shown the influence of retardation effects on electron angular distributions. A similar situation was found in Rayleigh scattering [16]. In this Letter, we show that in SCS, as in the usual Compton scattering [17,18], these effects cannot be neglected and that, more than this, they have important consequences on two-color ionization rates. More precisely, we show that by choosing appropriately the relative orientation of the photon beams, the rate for ionization by SCS can be increased by orders of magnitude.

As the two approaches mentioned before (TDSE and LOPT) have been shown to be efficient and complementary [15] to study retardation effects in the keV range for the one-color case, we appreciate that they are also sufficiently versatile to be extended to the present context.

In the Coulomb gauge the exact nonrelativistic Hamiltonian of the one-electron atom with fixed nucleus interacting with the external electromagnetic field described by the vector potential $\mathbf{A}$ can be written (in atomic units) as

$$\mathcal{H} = H_{\rm at} + \mathbf{A}(\mathbf{r},t)\cdot\mathbf{P} + \frac{1}{2}\mathbf{A}^2(\mathbf{r},t), \qquad \nabla\cdot\mathbf{A} = 0, \quad (1)$$

with $\mathbf{P}$ the momentum operator and $H_{\rm at} = \frac{1}{2}\mathbf{P}^2 + V(r)$ the atomic Hamiltonian, where $V(r)$ is the atomic potential. In the two-color case, considering that the two fields (1 and 2) are both linearly polarized along the same direction, taken as the $z$ axis, the vector potential is the sum of two terms of the form

$$\mathbf{A}_i(\mathbf{r},t) = A_i(t - \alpha\mathbf{n}_i\cdot\mathbf{r})\mathbf{e}_z, \qquad i = 1,2. \quad (2)$$

$\alpha$ is the fine-structure constant ($\alpha = 1/c$) and $\mathbf{n}_i$ is the propagating direction of the field $i$, which verifies the orthogonality condition $\mathbf{n}_i\cdot\mathbf{e}_z = 0$. In order to describe radiation pulses, each function $A_i$ has to be nonvanishing over a finite interval (equal to the total duration of the pulse) of its independent variable; as in our previous works [10,15], we choose a $\cos^2$ envelope for the shape of the pulses.

The numerical integration of the TDSE treating exactly the position dependence of $\mathbf{A}_i(\mathbf{r},t)$ is too demanding. Supposing that the region of small distances gives the dominant contribution to the response of the atom exposed to the x-ray pulse, it is justified to approximate the function $A_i(t - \alpha\mathbf{n}_i\cdot\mathbf{r})$ by the first two terms of its power series in $\mathbf{n}_i\cdot\mathbf{r}$,

$$A_i(t - \alpha\mathbf{n}_i\cdot\mathbf{r}) \approx A_i(t) + \alpha F_i(t)\mathbf{n}_i\cdot\mathbf{r}, \quad (3)$$

where $F_i(t) \equiv -\dot{A}_i(t)$. The necessary condition of validity of this approximation is $\alpha\omega_i < 1$ or, equivalently, $\omega_i < 3.73$ keV in the case of hydrogen. The approach fully neglects relativistic effects of $\mathcal{O}(1/c^2)$, which is reasonable for the photon energies considered here.

With the approximation (3) and the notation $A(t) \equiv A_1(t) + A_2(t)$, the Hamiltonian becomes

$$\mathcal{H} \approx \mathcal{H}_{\rm at} + \mathcal{H}^{(1)}_{\rm DA} + \mathcal{H}^{(1)}_{RET} + \mathcal{H}^{(2)}_{RET} \equiv \tilde{\mathcal{H}}. \quad (4)$$

The terms $\mathcal{H}^{(1)}_{\rm DA} = A(t)P_z$ and $\mathcal{H}^{(1)}_{RET} = \alpha F_a(t)xP_z + \alpha F_b(t)yP_z$ both originate from $\mathbf{A}\cdot\mathbf{P}$ in Eq. (1), while $\mathcal{H}^{(2)}_{RET} = \alpha F_a(t)A(t)x + \alpha F_b(t)A(t)y$ comes from the approximation of $\mathbf{A}^2$. Taking the propagation direction of the first pulse along $Ox$ and denoting the azimuthal angle of the second pulse direction by $\beta$, one has $F_a(t) = F_1(t) + F_2(t)\cos\beta$ and $F_b(t) = F_2(t)\sin\beta$. In dipole approximation (DA), the Hamiltonian reduces to $\mathcal{H}_{\rm DA} = \mathcal{H}_{\rm at} + \mathcal{H}^{(1)}_{\rm DA}$.

We integrate the TDSE with the Hamiltonian $\tilde{\mathcal{H}}$ given in Eq. (4) using a spectral method. Once the wave function $\psi(\mathbf{r},t)$, the solution of the TDSE, is known at the end of the pulse, the photoelectron distributions are extracted from it. See Ref. [10] for details regarding the numerical resolution of the TDSE.

Referring now to LOPT based on the exact Hamiltonian (1) for the case of two monochromatic fields (photon energies $\omega_1$ and $\omega_2$) , the $\mathbf{A}\cdot\mathbf{P}$ contribution in first order is responsible for one-photon transitions while $\mathbf{A}^2$, taken in first order, and the $\mathbf{A}\cdot\mathbf{P}$ term, taken in second order, contribute to two-photon transitions. Figure 1 shows a schematic representation of the SCS. The left-hand part of the figure corresponds to the second-order path diagrams of perturbation theory, involving the term $\mathbf{A}\cdot\mathbf{P}$. On path 1 the absorption of the frequency $\omega_1$ from the ground state is followed by the emission of the frequency $\omega_2$; path 2 represents the same virtual transition but in the reverse order. The figure also shows schematically the transition associated with $\mathbf{A}^2$. All three paths lead to the ionization of H($1s$) with a final electron energy close to $\omega_1 - \omega_2 - I_p$, where $I_p$ is the ionization potential (0.5 a.u. in the case of hydrogen). The matrix element of $\mathbf{A}^2$ vanishing in DA, its contribution reveals unambiguously the presence of retardation effects.

Figure 2 shows electron spectra for the case $\omega_1 = 55$ a.u., $\omega_2 = 50$ a.u. with the two fields propagating in the same direction ($\beta = 0$, upper panel) and in opposite directions ($\beta = \pi$, lower panel). The pulses are superposed in time and their duration is $6\pi$ a.u. (165 cycles for field 1 and 150 cycles for field 2). We choose a common peak intensity $I_1 = I_2 = I_0$, where $I_0 \approx 3.51\times10^{16}$ W/cm$^2$. As mentioned in the figure caption, the TDSE is numerically integrated in four cases: (i) with the Hamiltonian (4), and

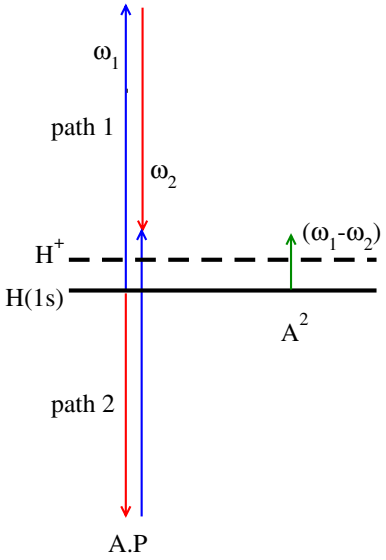


FIG. 1 (color online). A schematic diagram of the two-photon hydrogen ionization involving the absorption of photon $\omega_1$ and the emission of photon $\omega_2$. The horizontal dashed line represents the hydrogen ionization threshold. Left: Virtual transitions due to the second-order couplings via the operator $\mathbf{A}\cdot\mathbf{P}$. Right: Direct first-order transition due to the coupling via the operator $\mathbf{A}^2$.

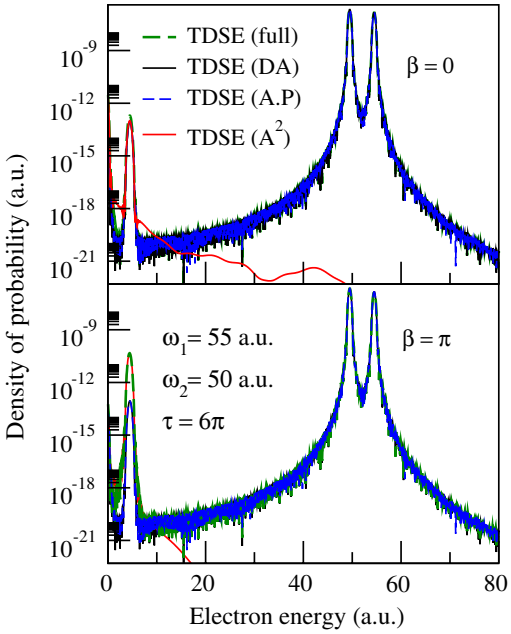


FIG. 2 (color online). Photoelectron spectra calculated with a peak intensity of $3.51\times10^{16}$ W/cm$^2$ for two pulses propagating in the same direction (upper panel) and two counterpropagating pulses (lower panel). Four different approximations for the resolution of the TDSE are shown; see the text.

within different approximations; (ii) with the dipole approximation; (iii) neglecting the last term in Eq. (4); and (iv) neglecting the $\mathbf{A}\cdot\mathbf{P}$ terms in Eq. (4). The four corresponding curves are labeled TDSE (full), TDSE (DA), TDSE (A.P), and TDSE ($A^2$), respectively.

Each panel displays three dominant peaks: the highest ones, close to 50 and 55 a.u., are associated with one-photon absorption (photon energy $\omega_1$ or $\omega_2$). Here we are interested in the peak located at 4.5 a.u. in which we identify the contribution of SCS. Before describing it, we note that the first two mentioned peaks are dominated by the DA contribution, the nondipole corrections, due to $\mathcal{H}^{(1)}_{RET}$, playing a minor role. Consequently, the three curves corresponding to cases (i)–(iii) almost coincide (in both panels) over a large energy interval around the peaks due to one-photon ionization.

Concerning the structure centered at 4.5 a.u., it is of particular interest to note that, for $\beta=0$, the contributions coming from DA (independent of $\beta$) and $A^2$ are of the same order of magnitude, while for $\beta=\pi$, the contribution of $\mathbf{A}^2$ clearly dominates: compared to the previous case, it has increased by more than 2 orders of magnitude. The curves TDSE (DA) and TDSE (A.P) are very close to each other around this peak in both panels, meaning that retardation corrections to the A.P contribution are small (similarly to the case of one-photon ionization). When passing from the upper panel to the lower panel, one sees that TDSE (full) and TDSE ($A^2$) curves detach from the others and become practically superimposed. In both cases the retardation cannot be neglected. The relative importance of $\mathbf{A}^2$ compared to DA is related to a partial cancellation of the contribution of the two absorption paths shown in the left-hand part of the diagram 1; this has been demonstrated in the context of Compton scattering in earlier calculations [17]. We note the structure close to threshold, which is also present in the one-color case [10], and it is due to the laser bandwidth.

Nondipole terms introduce new angular couplings in the partial wave decomposition of the wave function; in particular, the term associated with $\mathbf{A}^2$ couples states with $l'=l\pm1$ and $m'=m\pm1$. Their presence is reflected in the ejected electron angular distributions. Figure 3 shows electron angular distributions for the case $\beta=0$, corresponding to the region of the peak at 4.5 a.u. in the electron energy spectrum shown in the upper panel of Fig. 2. The differential probability was integrated within energies ranging from 2.3 to 6 a.u. The figure clearly shows that the shape of the angular distributions calculated with the full Hamiltonian and in DA totally differ, due to the influence of the term $\mathbf{A}^2$. In the case where the electron is ejected in the plane perpendicular to the propagation direction of the fields ($\varphi_e=\pi/2$, see figure), the DA angular distribution dominates, the contribution of $\mathbf{A}^2$ being zero for symmetry reasons.

At the pulse durations used here, we have found that SCS densities of probabilities extracted from the TDSE are approximately proportional to the pulse duration. Also, these densities vary quadratically with the intensity, as expected in the perturbative regime. Therefore, at longer

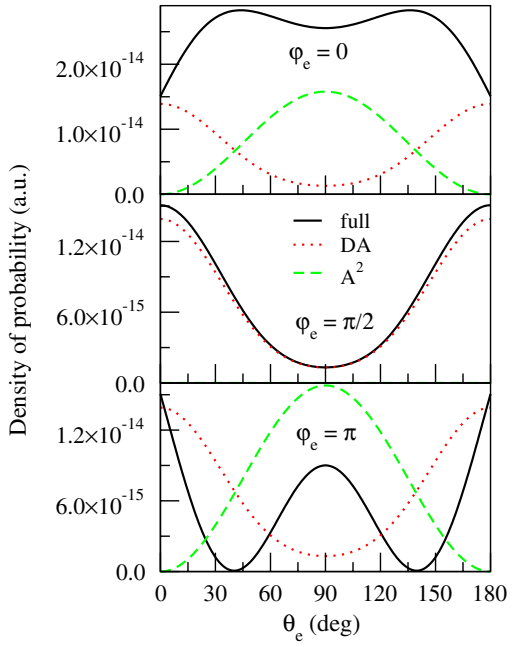


FIG. 3 (color online). Angular distributions of the electrons ejected by SCS [with energies around the maximum located at 4.5 a.u. (see Fig. 2)], for $\beta = 0$ (fields propagating in the same direction) versus the polar angle $\theta_e$ of the electron momentum for three different values of the azimuthal angle $\varphi_e$. The labels full, DA, and $A^2$ refer to TDSE calculations based on different approximations, as in Fig. 2; see the text.

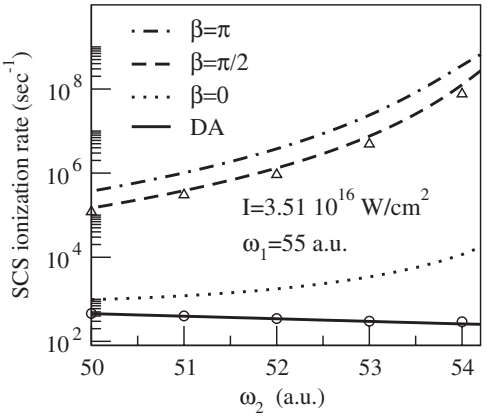


FIG. 4. Stimulated Compton scattering ionization rate, calculated in perturbation theory, versus the photon energy $\omega_2$ for an intensity of $3.51 \times 10^{16}$ W/cm$^2$ and $\omega_1 = 55$ a.u.. The propagation direction of the field 1 is along $Ox$ and $\beta = 0, \pi/2, \pi$. The figure also shows the rate calculated in DA. The triangles refer to rates extracted from full TDSE calculations (at $\beta = \pi/2$) and the circles refer to the rates extracted from TDSE in DA.

pulses durations, the main features of the spectra presented above are expected to remain unchanged, except for an overall increase of the ionization yields. The predictions of LOPT are easily obtained from the corresponding nonrelativistic matrix element including retardation [19]. In particular, the $\mathbf{A}^2$ contribution [14,20] comes from

$$\mathcal{O}(\mathbf{p}, \mathbf{K}) \equiv m_e c \sqrt{p} \langle \mathbf{p} - |e^{i\mathbf{K}\cdot\mathbf{r}}|1s\rangle, \tag{5}$$

with $\mathbf{p}$ the asymptotic momentum of the ejected electron and $\mathbf{K} = \kappa_1 - \kappa_2$ ($\kappa_1$ and $\kappa_2$ the photon momenta) the photon momentum transfer. The advantage of the perturbative approach is that the matrix element above has an exact analytical expression [19], as does the total cross section, obtained by integrating over the electron direction. In contrast to the TDSE approach, a power series expansion of the exponential $e^{i\mathbf{K}\cdot\mathbf{r}}$ [i.e., the equivalent of Eq. (3) in the LOPT approach] is not used to calculate the above matrix element.

In the case of two monochromatic electromagnetic plane waves, Fig. 4 presents the total ionization rate for SCS calculated in perturbation theory, based on the contributions of both $\mathbf{A}^2$ and $\mathbf{A}\cdot\mathbf{P}$ terms, the latter taken in DA. One frequency is fixed at $\omega_1 = 55$ a.u., while $\omega_2$ takes values from 50 to 54.25 a.u. The intensity was taken equal to the atomic unit $I_0$. Three propagation directions of the field 2 were considered: $\beta = 0$, $\beta = \pi/2$, and $\beta = \pi$. The inclusion of $\mathbf{A}\cdot\mathbf{P}$ only matters, however, for $\beta = 0$. We have checked that the ionization rates extracted from the TDSE calculations agree well with LOPT values; this is illustrated in Fig. 4 for the particular cases of $\beta = \pi/2$ and DA. The figure clearly exhibits the strong dependence of the ionization rate on the propagation angle $\beta$; in particular, the ionization probability is lowest for $\beta = 0$. Using LOPT, it is easy to show that the contribution of $\mathbf{A}^2$ to the ionization rate scales as $K^2 \propto \omega_1^2 + \omega_2^2 - 2\omega_1\omega_2 \cos\beta$. Owing to the values of $\omega_1$ and $\omega_2$, this simple relation explains why the signal increases sharply when $\beta$ is varied from 0 to $\pi$. Figure 4 also shows that the two-color ionization rate increases by several orders of magnitude when $\omega_2$ becomes close to $\omega_1$. On the basis of these findings, we have performed TDSE calculations for $\omega_1 = 55$ a.u., $\omega_2 = 53.5$ a.u., and an intensity of $10^{18}$ W/cm$^2$, and we have found that, indeed, the two-color ionization competes with one-photon ionization in the case of perpendicular propagation directions and even dominates for counterpropagating fields.

In conclusion, we have identified the presence of the SCS process in the electron energy and angular spectra associated with two-color ionization of hydrogen with keV photons using TDSE, at electron energies close to the difference of energies of the two photons. The results show that (i) the term $\mathbf{A}^2$ (a retardation contribution) competes with or even dominates the second-order contribution of $\mathbf{A}\cdot\mathbf{P}$, (ii) retardation effects are even stronger in the electron angular distributions, which is of particular interest from an experimental point of view, and (iii) as the angle between the propagation directions of the fields increases from 0 to $\pi$, SCS becomes more important. These effects are reflected in the ionization rates and angular distributions. At high intensity, SCS may dominate over one-photon ionization in the case of perpendicular propagation, then most of the ionization occurs within the field crossing

region. It is, therefore, of high interest to investigate two-color ionization processes at XFELs.

It is a pleasure to thank Philippe Balcou for discussions which led us to the problem addressed in this Letter. This work started with the support of the European COST Action CM0702. The authors thank the Université de Bordeaux for providing access to the Mésocentre de Calcul Intensif Aquitain (MCIA). We also acknowledge the support of the European Science Fundation Research Networking Progam SILMI and Contract No. 1 RNP/2012 from ANCS through CNCS-UEFISCDI.

[1] S. Jamison, Nat. Photonics **4**, 589 (2010).
[2] P. Emma *et al.*, Nat. Photonics **4**, 641 (2010).
[3] T. Shintake *et al.*, Nat. Photonics **2**, 555 (2008).
[4] T. Ishikawa *et al.*, Nat. Photonics **6**, 540 (2012).
[5] G. Doumy *et al.*, Phys. Rev. Lett. **106**, 083002 (2011).
[6] H. Fukuzawa *et al.*, Phys. Rev. Lett. **110**, 173005 (2013).
[7] A. A. Lutman, R. Coffee, Y. Ding, Z. Huang, J. Krzywinski, T. Maxwell, M. Messerschmidt, and H.-D. Nuhn, Phys. Rev. Lett. **110**, 134801 (2013).
[8] E. Schrödinger, Ann. Phys. (Leipzig) **82**, 257 (1927).
[9] P. L. Kapitza and P. A. M. Dirac, Proc. Cambridge Philos. Soc. **29**, 297 (1933)
[10] M. Dondera and H. Bachau, Phys. Rev. A **85**, 013423 (2012).
[11] L. V. Keldysh, Sov. Phys. JETP **20**, 1307 (1965).
[12] O. Hemmers, R. Guillemin, and D. V. Lidle, Radiat. Phys. Chem. **70**, 123 (2004).
[13] R. Guillemin *et al.*, Phys. Rev. Lett. **89**, 033002 (2002).
[14] V. Florescu, O. Budriga, and H. Bachau, Phys. Rev. A **86**, 033413 (2012).
[15] H. Bachau, O. Budriga, M. Dondera, and V. Florescu, Central Eur. J. Phys. **11**, 1091 (2013).
[16] L. Safari, P. Amaro, S. Fritzsche, J. P. Santos, and F. Fratini, Phys. Rev. A **85**, 043406 (2012).
[17] P. Eisenberger and P. M. Platzman, Phys. Rev. A **2**, 415 (1970).
[18] R. H. Pratt, L. A. Lajohn, V. Florescu, T. Surić, B. K. Chatterjee, and S. C. Roy, Radiat. Phys. Chem. **79**, 124 (2010).
[19] M. Gavrila, Phys. Rev. A **6**, 1348 (1972).
[20] V. Florescu, O. Budriga, and H. Bachau, Phys. Rev. A **84**, 033425 (2011).